JOURNAL OF MATERIALS SCIENCE 29 (1994) 824–829

Fracture toughness of $CaO–P_2O_5–B_2O_3$ glasses and glass-ceramics determined by indentation

WEIDONG SHI, P. F. JAMES
Department of Engineering Materials, The University of Sheffield, Sir Robert Hadfield Building, Mappin Street, Sheffield S1 4DU, UK

The fracture toughness, (K_{IC}) of $CaO–P_2O_5–B_2O_3$ glasses and glass-ceramics was investigated using both Vickers indentation and the notched beam technique (NBT). Five representative equations were applied and it was found that for the variation of K_{IC} with B_2O_3 content, the Lawn and Fuller equation showed the best correspondence with the NBT. The values of fracture toughness obtained from the Lawn and Fuller equation showed the same trend with B_2O_3 content as that determined by NBT, although the values from indentation were on average 33% lower. The determination of absolute fracture toughness by indentation requires a correction factor which can be obtained by calibration using NBT. A significant increase in K_{IC} occurred after a $37CaO–37P_2O_5–20B_2O_3–6Al_2O_3$ (mol %) glass was converted to a glass-ceramic. The much higher K_{IC} for the glass-ceramic measured by NBT (1.32 MN m$^{-3/2}$) compared with that from indentation (0.89 MN m$^{-3/2}$) is attributed to internal stresses due to thermal expansion differences between the crystalline and residual glass phases leading to additional microcrack toughening.

1. Introduction

The measurement of fracture toughness, or critical stress intensity factor, K_{IC}, of materials by established methods such as the notched beam technique (NBT) [1], requires a large number of samples and preparation of specimens of sufficient size and suitable shape. Such methods are difficult to use in the development of new materials on a laboratory scale, because in this case the fabricated samples are small. However, the determination of fracture toughness by the indentation technique allows many measurements on a single specimen so that detailed trends in toughness can be followed with small quantities of material. Since Palmqvist [2, 3] used indentation cracks to measure the fracture toughness of materials, several equations have been proposed and have been applied to different glasses and ceramics [4–9]. Attempts were made to obtain values of K_{IC} by relating the microfracture patterns in brittle solids to the contact load in terms of Young's modulus and microhardness. However, it is sometimes inconvenient to obtain both of these parameters when studying new materials.

In this work, five representative equations (developed by Lawn and Fuller [4], Evans and Charles [5], Lankford [6] and Niihara *et al.* [7–9]) were explored in order to assess the applicability of the Vickers indentation microfracture technique to the measurement of the fracture toughnesses of calcium phosphate-based glasses and glass-ceramics.

Lawn and Fuller [4] have provided a simple formulation for the well-developed stage of indentation fracture based on ideal "sharp indentor" geometry (see Fig. 1a). The extent of surface traces of well-developed median cracks can be related to the contact load, P, in terms of fracture toughness as follows

$$K_{IC} = \frac{P/c^{3/2}}{\pi^{3/2}\tan\psi} \quad (1)$$

where c is the crack length shown in Fig. 1a, ψ is the half-angle of the indentor (for a Vickers pyramid, $\psi = 68°$, the half-angle between opposing pyramid edges).

According to Evans and Charles [5], a dimensional analysis of indentation fracture has shown that the indentation crack length c, should be related to the impression radius, a, by

$$K_{IC}\phi/(Ha^{1/2}) = 0.15k'(c/a)^{-3/2} \quad (2)$$

where H is hardness, ϕ the constraint factor (~ 3), and k' is a correction factor ($= 3.2$).

Lankford [6] states that the fracture toughness for both the Palmqvist cracks and the radial cracks (for higher c/a ratios) can be obtained from a single equation

$$(K_{IC}\phi/Ha^{1/2})(H/E\phi)^{2/5} = 0.142(c/a)^{-1.56} \quad (3)$$

Niihara *et al.* [7–9] suggest that the fracture toughness, K_{IC}, can be calculated from experimental values of the half diagonal, a, of the indentation and the crack size, c, as follows. For ratios of $l/a > 2.0$, which were found at high values of indentation load (see Fig. 1a), K_{IC} was obtained from

$$(K_{IC}\phi/Ha^{1/2})(H/E\phi)^{2/5} = 0.129(c/a)^{-3/2} \quad (4)$$

For ratios of $l/a < 2.0$, (i.e. $c/a < 3.0$), which occurred at the lower values of load where Palmqvist cracks

0022–2461

TABLE I Glass compositions (mol %), and values of Youngs' modulus, E, and hardness, H, with standard deviations

Glass no	CaO	P_2O_5	B_2O_3	Al_2O_3	SiO_2	E(GPa)	H(GPa)
CPB1	47.5	47.5	5			32 ± 2.6	4.74 ± 0.28
CPB3	42.5	42.5	15			28 ± 3.1	5.07 ± 0.31
CPB4	40	40	20			32 ± 4.2	5.36 ± 0.29
CPB5	37.5	37.5	25			30 ± 3.8	5.6 ± 0.30
CPB6	32.5	32.5	35			29 ± 4.4	5.98 ± 0.27
CPBA10	37	37	20	6		–	–
CPBS12	37	37	20		6	–	–

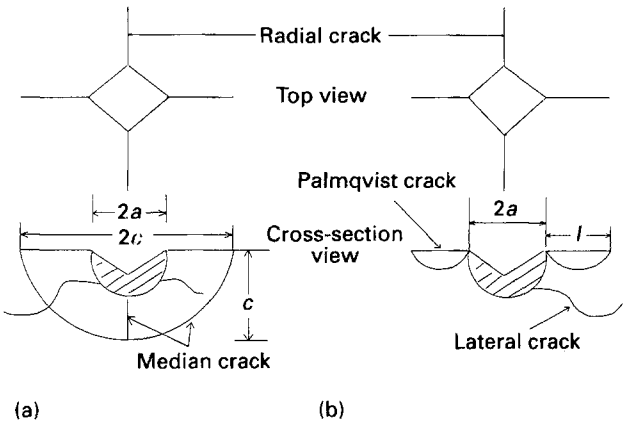

Figure 1 Top and cross-sectional views around Vickers indent assuming (a) median cracks and (b) Palmqvist cracks; plastic zone is represented by cross hatching.

were formed (see Fig. 1b), the appropriate expression was

$$(K_{IC}\phi/Ha^{1/2})(H/E\phi)^{2/5} = 0.035(l/a)^{-1/2} \quad (5)$$

where ϕ is a constraint factor (~ 3), H the Vickers hardness, and E is Young's modulus.

The fracture toughness results from Vickers indentation were compared with fracture toughness data obtained using the established notched beam technique in order to test the validity of the indentation method for the present phosphate glass system. For comparison, the fracture toughness of a canasite glass-ceramic was also measured using the indentation method because fracture toughness values obtained by the chevron-notched, short-bar, notched beam and indentation methods are available from published work [10].

The present work is part of a general investigation of the properties and crystallization behaviour of calcium phosphate-based systems. Glasses and glass-ceramics based on calcium phosphate have potential applications as biomedical materials. In previous papers, preparation of glass-ceramics in the $CaO–P_2O_5$ system using additions of Al_2O_3 and TiO_2 as nucleating agents was described [11], and the properties and crystallization of $CaO–P_2O_5–B_2O_3$ and $CaO–P_2O_5$ $B_2O_3–Al_2O_3$ glasses investigated [12–14].

2. Experimental procedure

The glasses were prepared from reagent-grade calcium hydrogen phosphate ($CaH_4(PO_4)_2 \cdot H_2O$, boric acid (H_3BO_3), aluminium hydroxide ($Al(OH)_3$) and pure silica sand (SiO_2). The premixed batches were sintered at 700 °C and melted in alumina crucibles at 1200–1420 °C for 2 h. The melts were poured on to a preheated graphite or steel plate. The final compositions are given in Table I. The molar percentages of CaO and P_2O_5 were equal in each glass, and the B_2O_3 content was varied from 5–35 mol %. Two of the glasses contained 6 mol % Al_2O_3 and 6 mol % SiO_2, respectively. The glass containing Al_2O_3 as a crystal nucleating agent (CPBA10) was converted to a glass-ceramic by heat treating at 680 °C for 1 h followed by 800 °C for 10 min.

Specimens about 5 mm thick were used for indentation experiments. All glasses were annealed at 560–600 °C for 2 h (glass transformation temperatures, T_g), used to define annealing temperatures are given in previous papers [12, 13] in order to release thermal stresses produced during the glass-casting process. After cooling slowly at 2 °C min^{-1} through the transformation range they were then examined in a polarized light stress detector to ensure that stresses were removed. Specimens were finely polished using SiC followed by diamond to 1 μm finish. Subsequently, any residual surface compression effects due to surface grinding were minimized by annealing the glasses again for 30 min, followed by slow cooling. A standard miniload microhardness tester with a Vickers diamond pyramid was used for indentation tests at room temperature. Five indentor loads of 1.47, 1.96, 2.94, 3.92 and 4.90 N were used for all specimens. With the specimen and diamond indentor in position (nearly touching), the indentor was released on to the specimen through a rate-control system. A loading rate of 8 mm min^{-1} was chosen for all measurements because a loading rate lower than 0.2–0.5 mm min^{-1} may induce different crack lengths caused by rate-dependent environmental effects [15]. After this process, the indentor was removed and replaced by a microscope. The surface traces of the cracks extending from the impression corners were measured by using the graticule in the optical microscope. A typical crack pattern obtained from a $CaO–P_2O_5–B_2O_3$ glass is illustrated in Fig. 2. For each load value, 13–16 separate indentations were made on each specimen surface.

A separate standard measurement of Vickers hardness, H, for each glass composition, required in the K_{IC} determinations by indentation, was made using the miniload tester. The mean diagonal length of ten impressions was measured at low loads where cracking did not occur, and H was obtained by the standard equation [16].

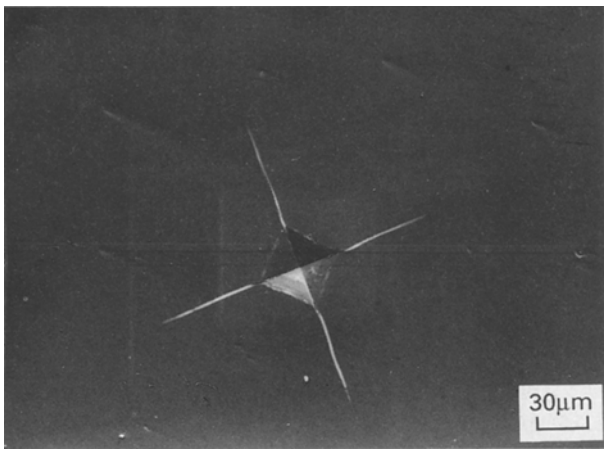

Figure 2 A typical crack pattern obtained from $CaO–P_2O_5–B_2O_3$ glass (CPB5) using Vickers indentation (scanning electron micrograph).

Specimens for K_{IC} measurements by the NBT were prepared in the form of rectangular bars, about 5.5 mm × 3 mm × 35 mm. One 35 mm edge of each specimen was V-notched with a diamond wheel and precrack lengths were measured by optical microscopy. Specimens were tested in three-point bending using a Mayes machine for a 20 mm span at a crosshead speed of 0.4 mm min^{-1}. K_{IC} was calculated using the following equation [1]:

$$K_{IC} = \frac{6Md^{1/2}}{bw^2} Y \quad (6)$$

where M is the applied bending moment at fracture, d is the notch depth and b, w are dimensions of cross-section of the rectangular bars. Y is a dimensionless parameter which depends on d/w and on type of loading. All measurements were carried out in air at room temperature. At least 12 specimens for each composition were tested. In addition, Young's moduli, E, for all the glasses, also required in K_{IC} determinations by indentation, were obtained by standard four-point bending experiments on unnotched beams [17]. Again, at least 12 specimens for each composition were used.

3. Results and discussion

According to Equations 1–5, K_{IC} measured under different indentation loads should be constant for a specific composition. However, this may not be the case in practice, because of residual thermal stress in the glass or the presence of a residual surface compression introduced by grinding. Table II gives values of fracture toughness, K_{IC}, determined from Equation 1 using specimens of unannealed glass at different indentation loads, P. The greater scatter of values compared with the result for the annealed glass (Table IV, to be discussed below) is probably caused by residual stresses in the glass. The values of K_{IC} in Table II are also lower than that in Table IV. The residual stresses cause an appreciable crack opening at zero load that facilitates the observation of the cracks in the optical microscope [18]. These stresses can be minimized by careful annealing but cannot be removed entirely and

TABLE II Results for unannealed glass CPBS12

Load	K_{IC} (MN $m^{-3/2}$)	Standard deviation (MN $m^{-3/2}$)
1.47	0.569	0.057
1.96	0.474	0.030
2.94	0.480	0.040
3.92	0.469	0.039

TABLE III Equations for K_{IC} measurement

Original equation	Proposed by	Plot used
$K_{IC} = \frac{P/c^{3/2}}{\pi^{3/2}\tan\psi}$	Lawn and Fuller [4] (Method 1)	$c^{3/2}$ versus P
$K_{IC} = 0.15\,H\frac{a^2}{c^{3/2}}$	Evans and Charles [5] Method 2	a^2 versus $c^{3/2}$
$K_{IC} = 0.0735\,E^{0.4} \times H^{0.6}\frac{a^{2.06}}{c^{1.56}}$	Lankford [6] Method 3	$a^{2.06}$ versus $c^{1.56}$
$K_{IC} = 0.0667\,E^{0.4} \times H^{0.6}\frac{a^2}{c^{3/2}}$	Niihara [7–9] Method 4	a^2 versus $c^{3/2}$
$K_{IC} = 0.0181\,E^{0.4} \times H^{0.6}\frac{a}{l^{0.5}}$	Niihara [7–9] Method 5	a versus $l^{0.5}$

a small variation in K_{IC} using different indentation loads is therefore expected. In addition, when using a low load, errors arise in measuring the short crack lengths produced. For this reason higher loads are preferable. Furthermore, the use of higher loads giving longer cracks eliminates the need for a highly polished surface. Another advantage of large cracks is that residual stresses very near the surface do not have as large an effect on the propagation of the median crack as they do for small cracks [15]. However, there is no clear criterion in the choice of a sufficiently high load for each material, especially in studying new materials. Therefore, a series of plots were made from the five equations discussed earlier, the slopes of the straight lines were determined by the least squares method and used to calculate K_{IC} values. The plots used are summarized in Table III. Five different indentor loads were used. The indentation results were analysed in terms of the various equations at face value, without attempting to determine the detailed cracking mechanism. Fig. 3 is a typical plot of $c^{3/2}$ against P for glass CPB5 using method 1 (Lawn and Fuller). For each load $\bar{c}^{3/2}$ is shown, where $\bar{c}$ is the mean crack length obtained from 13–16 individual measurements for each load. The upper and lower limits show the maximum and minimum values for each load and indicate the spread of observations. The best straight line was determined by least squares analysis using all the individual measurements, in this case 72, and the slope was used to calculate K_{IC} from the equation in Table III. Similar results to Fig. 3 were obtained for the other compositions. The plots for CPB1, CPB3, CPB4 and CPB6 are given in Fig. 4. The straight lines were

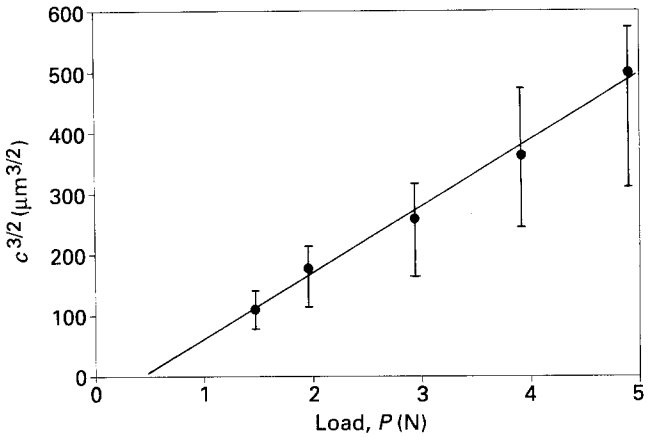

Figure 3 $C^{3/2}$ versus indentor load, P, in CPB5 glass. The upper and lower limits show the maximum and minimum values for each load, and indicate the spread of observations.

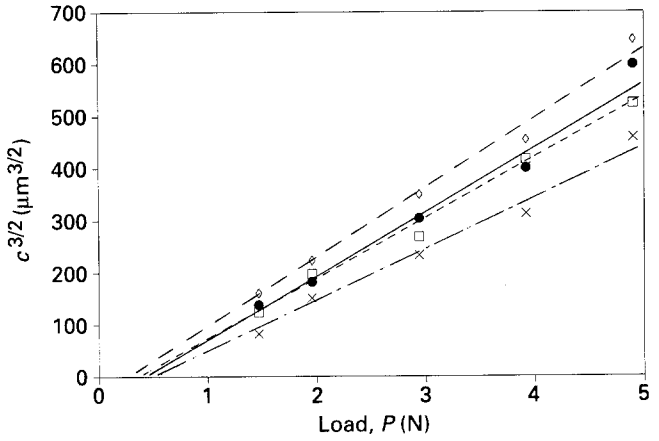

Figure 4 Plots for Lawn and Fuller method (method 1) in CPB glasses. (●) CPB1, (◇) CPB3, (□) CPB4, (×) CPB6.

determined by least squares analysis from all the observations as in Fig. 3, but for simplicity the points shown correspond to the mean crack length only. For the other four methods, the plots are given in Figs 5–7. The a^2 versus $c^{3/2}$ plot in Fig. 5 was used for the analyses with both methods 2 and 4. A significant feature of all the plots in Figs 3 and 4 is the positive intercept on the load axis. This positive intercept means that a minimum load must be applied in order to initiate the indentation crack on the surface. However, the intercept and the slope of plots of $c^{3/2}$ versus P can be changed by residual stresses [15]. In Fig. 8, the final fracture toughness values calculated from the different equations are plotted against B_2O_3 content in the $(50 - x/2)CaO$–$(50 - x/2)P_2O_5$–xB_2O_3 glass system. The fracture toughness obtained by NBT is also shown for comparison.

From Fig. 8, all the indentation methods give values typically 10%–30% lower than obtained by NBT. With regard to the relative trend of K_{IC} with B_2O_3 content, the Lawn and Fuller equation (method 1) shows the best correspondence with NBT; the results from method 1 are on average 33% lower than those using NBT (Tables IV and V). Both sets of results show the same trend of a small but gradual increase in fracture toughness with increase in B_2O_3 content (see Fig. 9).

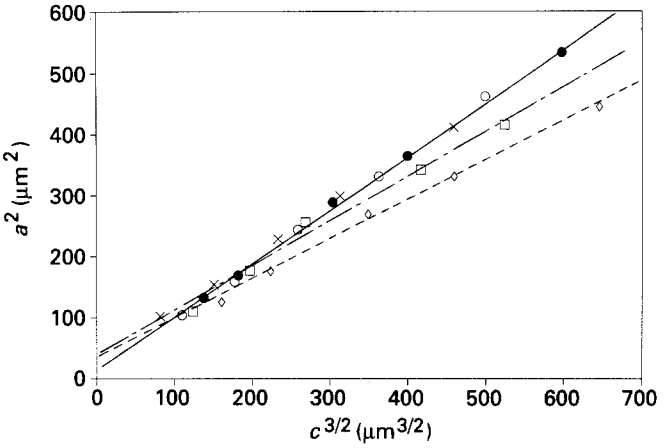

Figure 5 Plots for Evans and Charles method (method 2) in CPB glasses. The lines for CPB5, CPB6 are not included to avoid confusion; (●) CPB1, (◇) CPB3, (□) CPB4, (○) CPB5, (×) CPB6. The same plots were also used for the Niihara-1 method (method 4), see Table III.

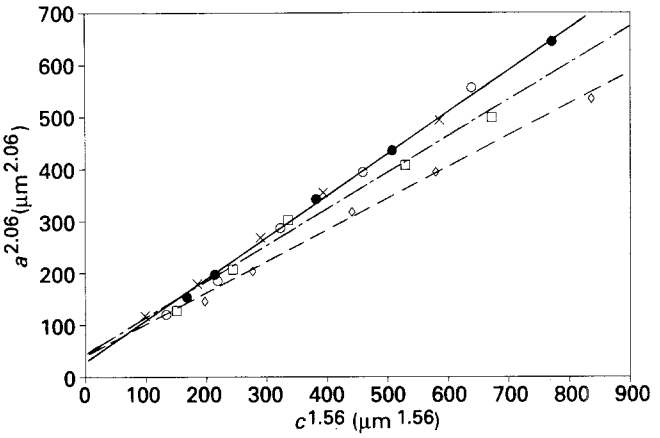

Figure 6 Plots for Lankford method (method 3) in CPB glasses. Lines for CPB5, CPB6 are not included to avoid confusion. (●) CPB1, (◇) CPB3, (□) CPB4, (○) CPB5, (×) CPB6.

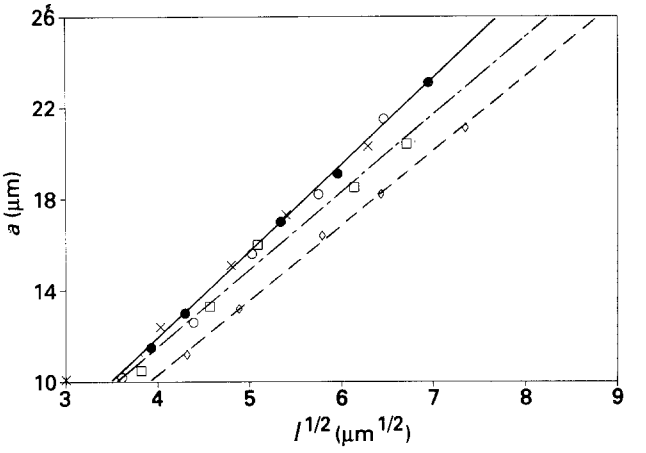

Figure 7 Plots for Niihara-2 method (method 5) in CPB glasses. Lines for CPB5, CPB6 are not included to avoid confusion. (●) CPB1, (◇) CPB3, (□) CPB4, (○) CPB5, (×) CPB6.

The present results demonstrate that indentation fracture is useful in obtaining a ranking of the fracture toughness, but that the values are lower than those determined by the established notched beam method based on fracture mechanics. Because of its simplicity,

TABLE IV Fracture toughness from indentation (method 1)

Glass no	No of measurements	K_{IC} (MN m$^{-3/2}$)	Standard deviation (MN m$^{-3/2}$)
CPB1	79	0.554	0.022
CPB3	77	0.537	0.015
CPB4	75	0.626	0.026
CPB5	72	0.666	0.032
CPB6	73	0.704	0.030
CPBS12	72	0.590	0.036
CPBA10	76	0.711	0.021
CPBA10[a]	71	0.890	0.049
Canasite	64	1.56	0.118

[a] Heat treated at 680 °C for 1 h followed by 800 °C for 10 min.

TABLE V Fracture toughness from three-point measurements using NBT

Glass no[a]	K_{IC} (MN m$^{-3/2}$)	Standard deviation (MN m$^{-3/2}$)
CPB1	0.772	0.031
CPB3	0.776	0.025
CPB4	0.799	0.013
CPB5	0.892	0.015
CPB6	0.918	0.020
CPBS12	0.777	0.034
CPBA10	0.902	0.0097
CPBA10[b]	1.32	0.032

[a] Number of measurements was 12.
[b] Heat treated at 680 °C for 1 h followed by 800 °C for 10 min.

method 1 (Lawn and Fuller) is preferable for rapid evaluation of the fracture toughness. For the other four modified equations (methods 2–4), either microhardness, H, or both Young's modulus, E, and H are included in the calculation. Hence the determination of E and H also introduces some errors into the calculation of K_{IC}. For method 1 (Lawn and Fuller), the absolute determination of fracture toughness by indentation requires a knowledge of a correction factor, k. In this case K_{IC} is calculated using the following equation [1]

$$K_{IC} = \frac{1}{k\pi^{3/2}\tan\psi(\text{slope})} \quad (7)$$

where the slope refers to the plot of $c^{3/2}$ versus P (Table III). Silicate glasses show values of the dimensionless constant $k\pi^{3/2}\tan\psi$ in the range 12–17.5 [15, 19]. The average value for the present CaO–P_2O_5–B_2O_3 glasses is significantly lower (10.1).

Results were reported recently for canasite (silicate) glass-ceramics [10] which showed that the fracture toughness values obtained by the direct measurement of the size of the indentation crack were appreciably lower than the values obtained by the chevron-notch, short-bar and notched beam methods over the total range of indentation loads and corresponding crack sizes. For example, K_{IC} was between 1 and 2 MN m$^{-3/2}$ using the indentation method and 4–5 MN m$^{-3/2}$ using the other methods. A sample of canasite glass ceramic was also measured for fracture toughness in this work. The result for K_{IC} by the indentation method (Table IV) was 1.56 MN m$^{-3/2}$ in close agreement with the results of Beall *et al.* [10]. The present results also indicate a significant increase in K_{IC} after the crystallization treatment of glass CPBA10 to convert it to a glass ceramic. Also the fracture toughness value obtained from indentation was much lower than that obtained by the notched beam method (0.89 MN m$^{-3/2}$ for indentation compared with 1.32 MN m$^{-3/2}$ for the notched beam test).

Beall *et al.* [10] explained the large difference in fracture toughness values for canasite glass-ceramic, obtained by indentation and from the methods (including NBT) in which samples were fractured to failure, in terms of the mechanisms of toughening and the effect of the test method. In particular, it was thought that there were differences in the distribution of the stress fields in the vicinity of the cracks between the indentation and other methods. Two primary mechanisms of toughening for canasite were discussed. The first mechanism was crack deflection, arising from the combined effects of the acicular microstructure and the preferred cleavage fracture. The second mechanism was stress-induced microcrack toughening, owing to the internal stresses caused by the anisotropy in thermal expansion of the individual

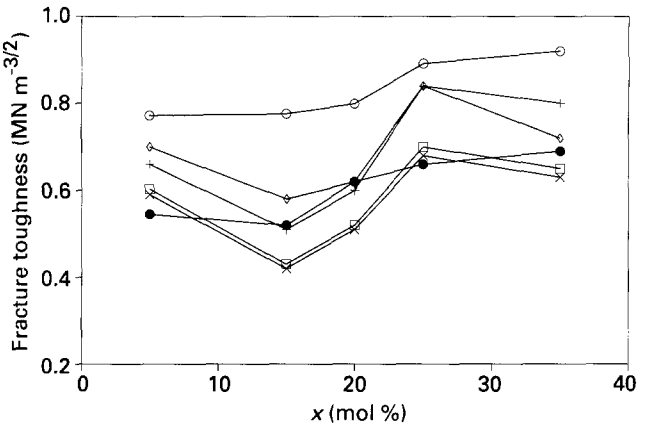

Figure 8 Fracture toughness measured by NBT and indentation methods in (50 − x/2)CaO–(50 − x/2)P_2O_5–xB_2O_3 glasses plotted against x (mol % B_2O_3). (○) NBT, and methods (●) 1, (+) 2, (□) 3, (×) 4, (◇) 5.

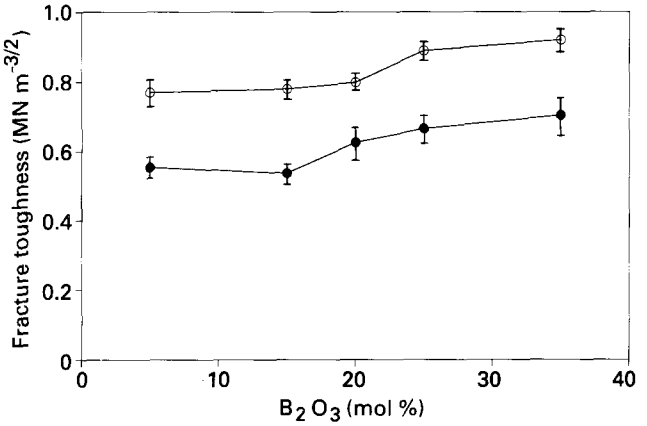

Figure 9 Fracture toughness measured by indentation (method 1) and NBT in (50 − x/2)CaO–(50 − x/2)P_2O_5–xB_2O_3 glasses plotted against x (mol % B_2O_3). Error bars indicate standard deviations about mean values. (●) indentation, (○) NBT.

crystals, leading to the microcracking by intergranular or intragranular cleavage fracture. It was suggested that although toughening by crack deflection may play a role at room temperature, microcrack toughening makes the major contribution to the observed value of fracture toughness. Moreover, microcrack toughening would be fully effective in the notch test, but largely suppressed in the indentation method. It was further suggested that for any toughening mechanism which relied on a stress-induced process, such as microcrack toughening or transformation toughening, the fracture toughness obtained by the indentation fracture method should be less than the corresponding value obtained by using other methods which relied on the onset of failure or extended crack propagation.

The above arguments may also help to explain the relatively large difference in K_{IC} values obtained by both indentation fracture and NBT for the CPBA10 glass ceramics. The notched beam method gave values approximately 50% larger than those from the indentation method, although the difference observed was not as large as that found for the canasite glass-ceramics. This glass-ceramic was more than 80% crystalline from XRD, the remainder consisting of glassy phase. The thermal expansion coefficient for the CPBA10 glass ceramic ($108 \times 10^{-7}\,°C^{-1}$) is significantly higher than that for the parent glass ($77 \times 10^{-7}\,°C^{-1}$). Therefore, significant residual stresses are expected in the glass ceramic on cooling to room temperature. The stresses would be expected to be predominantly compressive in the glass phase, and might lead to additional microcrack toughening in the CPBA10 glass-ceramic and explain the much higher K_{IC} value for NBT.

4. Conclusions

Fracture toughness, K_{IC}, was measured using five different equations by the indentation method in CaO–P_2O_5–B_2O_3 glasses and glass ceramics. It was found that the K_{IC} was sensitive to indentation load partly because of residual surface stresses in the samples. In practice, small fluctuations in fracture toughness could still be observed with different indentation loads, even after the samples were well annealed. A modified method of K_{IC} determination for the five equations was proposed using the slopes of the various plots, for example the slope of $c^{3/2}$ versus load, P, instead of using a single ratio of $P/c^{3/2}$ to determine a value of K_{IC}. The established notched beam technique (NBT) was used to measure K_{IC} for comparison with the values obtained by the indentation method. Method 1 using the Lawn and Fuller equation appeared to give the best description of the results, because it showed the same trend of K_{IC} with B_2O_3 as that obtained by NBT. On average the results were 33% lower than those obtained by NBT. Owing to the simplicity of this equation, method 1 is preferable for the rapid evaluation of fracture toughness. The other four equations must include either microhardness, H, or both Young's modulus, E, and H, and it may be difficult to obtain both these parameters in a laboratory-scale experiment when the samples are small. For toughness measurements using NBT a number of test specimens have to be prepared from each sample. The indentation technique allows many measurements on a single specimen so that detailed trends in toughness can be followed with small quantities of materials. However, it is clearly important where possible to check the values from indentation measurements against the notched beam method particularly if toughening related to a stress-induced process, such as microcrack toughening is suspected, as shown for certain glass-ceramics such as those based on canasite.

References

1. G. K. BANSAL and W. H. DUCKWORTH, in "Fracture Mechanics applied to Brittle Materials", Proceedings of the Eleventh National Symposium on Fracture Mechanics, Part II, ASTM STP678 edited by S. W. Freiman, (American Society for Testing and Materials, Philadelphia, PA, 1979), p. 38–46.
2. S. PALMQVIST, *Arch. Eisenhuttenw.* **33** (1962) 629.
3. *Idem, Jernk. Annal.* **167** (1963) 208.
4. B. R. LAWN and E. R. FULLER, *J. Mater. Sci.* **10** (1975) 2016.
5. A. G. EVANS and E. A. CHARLES, *J. Am. Ceram. Soc.* **59** (1976) 371.
6. J. LANKFORD, *J. Mater. Sci. Lett.* **1** (1982) 493.
7. K. NIIHARA, R. MORENA and D. P. H. HASSELMAN, *J. Mater. Sci. Lett.* **1** (1982) 13.
8. K. NIIHARA, R. MORENA and D. P. H. HASSELMAN, in "Fracture Mechanics of Ceramics", Vol. 5, edited by R. C. Bradt, A. G. Evans, D. P. H. Hasselman and F. F. Lange (Plenum, New York, 1983) p. 97.
9. K. NIIHARA, R. MORENA and D. P. H. HASSELMAN, *J. Am. Ceram. Soc.* **65** (7) (1982) C-116.
10. G. H. BEALL, K. CHYUNG, R. L. STEWART, K. Y. DONALDSON, H. L. LEE, S. BASKARAN and D. P. H. HASSELMAN, *J. Mater. Sci.* **21** (1986) 2365.
11. T. WANG and P. F. JAMES, in "New Materials and their Applications" edited by D. Holland, Institute of Physics Conference Series, no. 111 (IOP Publishing Ltd, Bristol, UK, 1990) p. 401.
12. W. SHI and P. F. JAMES, "Proceedings of the Int. Conf. on Physics of Non-crystalline Solids", edited by L. D. Pye, W. C. Lacourse and H. J. Stevens (Taylor and Francis, London, 1992) p. 401.
13. W. SHI and P. F. JAMES, *J. Mater. Sci.* **28** (1993) 469.
14. W. SHI, PhD Thesis, University of Sheffield, UK (1992).
15. R. H. MARION, in "Fracture Mechanics Applied to Brittle Materials", Proceedings of the Eleventh National Symposium on Fracture Mechanics, Part II, ASTM STP 678, edited by S. W. Freiman (American Society for Testing and Materials, Philadelphia, PA, 1979) p. 103–11.
16. D. G. HOLLOWAY, The Physical Properties of Glass", (Wykeham, London, 1973) p. 144.
17. J. M. GERE and S. P. TEMOSHENKO, "Mechanics of Materials" (Wadsworth International, Boston, 1985).
18. A. G. EVANS, in "Fracture Mechanics Applied to Brittle Materials", ASTM STP 678, edited by S. W. Freiman (American Society for Testing and Materials, Philadelphia, PA, 1979) p. 112–35.
19. D. B. MARSHALL and B. R. LAWN, *J. Am. Ceram. Soc.* **61** (1978) 21.

Received 15 April 1993
and accepted 3 June 1993